

# Dephasing due to nuclear spins in large-amplitude electric dipole spin resonance

Stefano Chesi,<sup>1,\*</sup> Li-Ping Yang,<sup>1</sup> and Daniel Loss<sup>2,3</sup>

<sup>1</sup>Beijing Computational Science Research Center, Beijing 100084, China

<sup>2</sup>Department of Physics, University of Basel, Basel, Switzerland

<sup>3</sup>CEMS, RIKEN, Wako, Saitama 351-0198, Japan

(Dated: December 26, 2021)

We have analyzed effects of the hyperfine interaction on electric dipole spin resonance when the amplitude of the quantum-dot motion becomes comparable or larger than the quantum dot's size. Away from the well known small-drive regime, transverse nuclear fluctuations become dominant and lead to a gaussian decay with characteristic dependence on drive strength and detuning. Based on our theory, we analyze recent electric-dipole spin resonance experiments relying on spin-orbit interactions or the slanting field of a micromagnet. We find that such experiments are already in a regime with significant effects of transverse nuclear fluctuations and the form of decay of the Rabi oscillations can be reproduced well by our theory.

PACS numbers: 85.35.Be, 75.75.-c, 76.30.-v, 03.65.Yz

*Introduction.* The interest in coherent manipulation of single electron spins has stimulated intense research efforts, leading to a great degree of control in a variety of nanostructures [1, 2]. For electrons in quantum dots, electron spin resonance (ESR) was first demonstrated in Ref. [3]. However, full electric control of local spins might be a better strategy for complex architectures of many quantum dots (envisioned to realize quantum information processing [4]). Thus, electric dipole spin resonance (EDSR) was developed relying on either spin-orbit couplings [5, 6] or the inhomogeneous magnetic field induced by a micromagnet [7, 8]. The effectiveness of EDSR is highlighted by recent experiments, which could demonstrate Rabi oscillations with frequencies larger than 100 MHz for both approaches [9, 10]. To further improve the performance of such spin manipulation schemes, it is important to characterize relevant dephasing mechanisms, and especially those which might become dominant at strong electric drive (i.e., fast Rabi frequency).

Hyperfine interactions are well known to play an important role in the electron spin dynamics of quantum dots. In particular, the ESR dephasing was successfully interpreted in terms of a static Overhauser field, with a variance of a few mT in GaAs. The resulting power-law decay and a universal  $\pi/4$  phase shift of the Rabi oscillations were accurately verified [11]. While EDSR experiments were also generally interpreted assuming a power-law decay, the expected  $t^{-1/2}$  dependence is violated at the larger values of the drive [9, 10, 12]. Recently, Ref. [10] has demonstrated striking deviations from the ESR behavior, including a crossover from the known power-law to a gaussian decay. Motivated by these findings, we re-examine here the theory of EDSR dephasing induced by the hyperfine interaction [11, 13], paying special attention to the regime of large-amplitude motion.

*Model.* EDSR is induced by a driven periodic displacement of the quantum dot  $\vec{R}(t) = \hat{e}_x \delta R \sin \omega t$ , which we take conventionally along  $x$ . For the time-dependent

wavefunction  $\psi(\vec{r} - \vec{R}(t))$ , we assume harmonic confinement along the direction of motion (which is applicable to both nanowire and lateral quantum dots):

$$|\psi(\vec{r})|^2 = |\varphi(y, z)|^2 \frac{1}{\sqrt{\pi} \delta x} e^{-x^2/\delta x^2}. \quad (1)$$

The spin dynamics can be described with the following Hamiltonian:

$$H = \frac{\epsilon_z}{2} \sigma_z + \frac{\vec{b} \cdot \vec{\sigma}}{2} \sin \omega t + \sum_i \frac{A_i}{n_0} \left| \psi(\vec{r}_i - \vec{R}(t)) \right|^2 \vec{\sigma} \cdot \vec{I}_i, \quad (2)$$

where the first term is the electron Zeeman coupling, with  $\epsilon_z = g\mu_B B$  and  $\vec{\sigma}$  the Pauli matrices. The second term is the drive, for which we can generally assume  $b \propto \delta R$  while other features (e.g., the direction of  $\vec{b}$ ) depend on specific details of the spin-orbit coupling or magnetic gradient. The last term in Eq. (2) is the Fermi contact hyperfine interaction, where  $n_0$  is the nuclear density.  $\vec{I}_i$  is the spin operator of nucleus  $i$ , with position  $\vec{r}_i$  and coupling  $A_i$ . The periodic time-dependence of Eq. (2) is characterized by Fourier components  $\psi_m(\vec{r}) = \frac{\omega}{2\pi} \int_0^{2\pi/\omega} |\psi(\vec{r} - \vec{R}(t))|^2 e^{-im\omega t} dt$ , of which only the static ( $m = 0$ ) and resonant ( $m = \pm 1$ ) ones are of interest here. In fact, in a frame rotating at frequency  $\omega \simeq \epsilon_z/\hbar$  and neglecting fast oscillating terms, the transformed Hamiltonian  $H'$  reads:

$$H' \simeq \frac{\epsilon_z - \hbar\omega}{2} \sigma_z - \frac{1}{4} (\vec{b} \times \vec{\sigma})_z + \sum_i \frac{A_i}{n_0} \left[ \psi_0(\vec{r}_i) \sigma_z I_{i,z} + i\psi_1(\vec{r}_i) (\vec{\sigma} \times \vec{I})_z \right], \quad (3)$$

where longitudinal/transverse fluctuations are controlled by  $\psi_0(\vec{r})$  and  $\psi_1(\vec{r})$ , respectively. Without loss of generality, we restrict ourselves to the case  $b_x = b_z = 0$  [14]:

$$H' = \frac{\Delta}{2} \sigma_z + \frac{b}{4} \sigma_x + \frac{1}{2} \vec{h} \cdot \vec{\sigma}, \quad (4)$$

where  $\Delta = \epsilon_z - \hbar\omega$  is the detuning and  $\vec{h}$  is defined by the second line of Eq. (3).

*Nuclear fluctuations.* On the relatively short time scales of the EDSR experiments, it is appropriate to describe  $\vec{h}$  with a static random classical magnetic field. In the lab frame and for infinite-temperature nuclear spins, the variance of the Overhauser field is given by  $\sigma^2 = \sum_i (2A_i/n_0)^2 |\psi(\vec{r}_i)|^4 I_i(I_i + 1)/3$ . However,  $\vec{h}$  is for a reference frame moving with the dot and rotating at frequency  $\omega$ . As a consequence, its statistical properties differ from the ones in the lab frame. We still have  $\langle \vec{h} \rangle = 0$ , but Eq. (3) implies that  $\langle h_z^2 \rangle$ ,  $\langle h_{x,y}^2 \rangle$  have an interesting dependence on the strength of the drive. For finite  $\delta R$  and  $|\psi(\vec{r})|^2$  as in Eq. (1) we can evaluate  $\langle h_z^2 \rangle$ ,  $\langle h_{x,y}^2 \rangle$  as follows, in terms of Hypergeometric functions:

$$\delta h_z = \frac{\sqrt{\langle h_z^2 \rangle}}{\sigma} = \sqrt{{}_pF_q\left(\frac{1}{2}, \frac{1}{2}; 1, 1; -\frac{2\delta R^2}{\delta x^2}\right)}, \quad (5)$$

$$\delta h_{xy} = \frac{\sqrt{\langle h_{x,y}^2 \rangle}}{\sigma} = \frac{1}{2} \frac{\delta R}{\delta x} \sqrt{{}_pF_q\left(\frac{3}{2}, \frac{3}{2}; 2, 3; -\frac{2\delta R^2}{\delta x^2}\right)}. \quad (6)$$

In the above formulas, the only dependence is on  $\delta R/\delta x$ , i.e., the amplitude of motion relative to the width of the electron wavefunction.  $\delta h_z$  and  $\delta h_{xy}$  are plotted in Fig. 1(a), showing that for  $\delta R \rightarrow 0$  only the longitudinal fluctuations survive. Therefore, in this limit one recovers the same behaviour of ESR. At finite  $\delta R/\delta x$ , the value of  $\delta h_z$  is a decreasing function of amplitude while the transverse fluctuations become non-zero and have a non-monotonic dependence on  $\delta R/\delta x$ . Such transverse fluctuations can serve at  $b = 0$  as a driving term [15], and in this context were previously discussed through an expansion at small  $\delta R$  [13] or numerical evaluation [16]. However, EDSR (both if driven through the slanting field of a micromagnet or spin-orbit interactions) is in a distinct physical regime than Refs. [13, 15, 16], because  $\delta h_{xy}$  is typically much smaller than the drive  $b$ . To see this, we notice that Eq. (6) implies  $\delta h_{xy} < \frac{1}{2} \delta R/\delta x$ , thus:

$$\frac{h_{x,y}}{b} \sim \frac{\sigma \delta h_{xy}}{b} < \frac{\delta R/\delta x}{2b/\sigma} = \frac{\eta}{2} \ll 1. \quad (7)$$

In Eq. (7) we defined the useful parameter  $\eta = \sigma \delta R/b\delta x$ .  $\eta$  is approximately constant (since  $b \propto \delta R$ ) and is typically small, according to our later estimates. Therefore, transverse nuclear fluctuations provide an additional dephasing mechanism which becomes progressively more important, until the maximum effect is reached at  $\delta R/\delta x \simeq 1.8$ . We will discuss how the effect of  $\delta h_{xy}$  becomes dominant over  $\delta h_z$  in a regime of sufficiently strong EDSR drive, which was already realized by recent experiments [10].

*Rabi oscillations.* We now use Eq. (5) and (6) to perform a gaussian average  $\overline{P_\downarrow(t)}$  with respect to  $\vec{h}$  of the

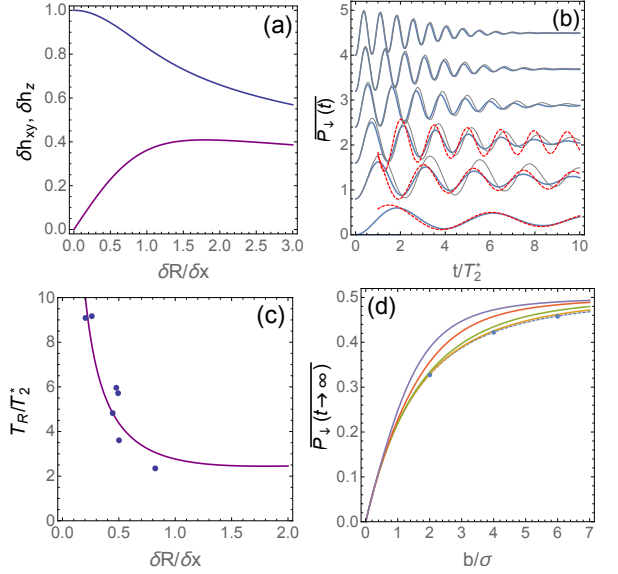


FIG. 1. (a): Plot of Eqs. (5) and (6), which characterize the longitudinal/transverse nuclear fluctuations (upper/lower curve, respectively). (b): Numerical result for the Rabi oscillations  $P_\downarrow(t)$ , averaged over nuclear fluctuations (blue thick curves). We used  $\eta = 0.05$ ,  $\Delta = 0$ , and  $\delta R/\delta x = 0.1, 0.2, \dots, 0.6$  (bottom to top). For clarity, the curves are shifted vertically. The red dashed curves are the asymptotic power-law decay of Ref. [11], valid when  $\delta R/\delta x \lesssim \sqrt{2\eta} \approx 0.3$ . The thin gray curves are from Eq. (9). (c): Plot of Eq. (11). Dots are decay times from Ref. [10], rescaled using  $T_2^* \simeq 9$  ns and  $\eta \simeq 0.09$ . (d): Large-time limit of  $\overline{P_\downarrow(t)}$ , plotted for  $\eta = 0.05, 0.1, 0.2, 0.5, 1$  (bottom to top). The dots on the dashed curve ( $\eta = 0.05$ ) refer to the three lowest curves of panel (b). On the scale of this plot, the dashed curve is indistinguishable from the  $\eta = 0$  limit.

spin-flip probability  $P_\downarrow(t)$ :

$$P_\downarrow(t) = \frac{(b/2 + h_x)^2 + h_y^2}{(b/2 + h_x)^2 + h_y^2 + (\Delta + h_z)^2} \times \sin^2 \left( \frac{t}{2\hbar} \sqrt{(b/2 + h_x)^2 + h_y^2 + (\Delta + h_z)^2} \right). \quad (8)$$

Although we cannot provide a general closed-form result, several relevant features can be explicitly characterized. In particular, at sufficiently large drive and detuning we can neglect the components of  $\vec{h}$  perpendicular to  $(b/2)\hat{e}_x + \Delta\hat{e}_z$  [see Eq. (4)], to obtain:

$$\overline{P_\downarrow(t)} \simeq \frac{b^2/2}{b^2 + 4\Delta^2} \left[ 1 - e^{-(t/T_R)^2} \cos \left( \frac{t}{\hbar} \sqrt{b^2/4 + \Delta^2} \right) \right]. \quad (9)$$

The Rabi decay time is:

$$T_R(\Delta) = \left( \frac{T_2^*}{\delta h_{xy}} \right) \times \sqrt{\frac{b^2 + 4\Delta^2}{b^2 + 4\Delta^2(\delta h_z/\delta h_{xy})^2}}, \quad (10)$$

with  $T_2^* = \sqrt{2}\hbar/\sigma$  the typical inhomogeneous dephasing time associated with nuclear spins. Equation (9) implies

a crossover between the ESR power-law decay at weak drive to the gaussian decay of the strong-drive regime.

To exemplify this behavior, we first consider the resonant condition ( $\Delta = 0$ ) when, besides  $\delta R/\delta x$ , the form of the decay is determined by  $T_2^*$  and the coefficient  $\eta$ . An example of numerical results for  $\overline{P_\downarrow(t)}$  is shown in Fig. 1(b), assuming  $\eta = 0.05$ . We confirm that the ESR power-law decay [3, 11] is recovered when  $\delta R/\delta x \rightarrow 0$  but significant deviations from this known dependence appear at larger strength of the drive. In the large-drive limit, we find a gaussian decay with no universal  $\pi/4$  phase shift, as Eq. (9) becomes an excellent approximation. Of special interest is the decay timescale, which simply follows from Eq. (10):

$$T_R(\Delta = 0) = \frac{T_2^*}{\delta h_{xy}}, \quad (11)$$

and is plotted in Fig. 1(c). The increasing strength of  $\delta h_x$  with the drive leads to a significantly faster decay, as also seen in the time domain results of Fig. 1(b).

The crossover to the strong-drive regime occurs when the effect of  $h_x$  in Eq. (8) becomes dominant over  $h_z$ , i.e.,  $b h_x \gg h_z^2$ . We estimate the typical values of  $h_x, h_z$  using the limit of  $\delta h_{xy}, \delta h_z$  at small  $\delta R/\delta x$  (which is justified if  $\eta \ll 1$ ), i.e.,  $h_x \sim \frac{1}{2}\sigma\delta R/\delta x$  and  $h_z \sim \sigma$ . This yields the condition:

$$\frac{\delta R}{\delta x} \gtrsim \sqrt{2\eta}, \quad (12)$$

which is in good agreement with the numerical results of Fig. 1(b).

*Stationary limit.* The long-time value  $\overline{P_\downarrow(t \rightarrow \infty)}$  is useful to estimate  $\sigma$ , either from the drive dependence at resonance (as done in the ESR experiment of Ref. [11]) or from the linewidth (considering finite detunings). Taking  $\Delta = 0$  in Eq. (9) gives  $\overline{P_\downarrow(\infty)} \simeq 1/2$  in the large-drive regime, thus the interesting drive dependence of  $\overline{P_\downarrow(\infty)}$  occurs when  $h_{x,y}$  are smaller than  $b, h_z$ . By neglecting in Eq. (8) such transverse nuclear fluctuations, we obtain the following expression:

$$\overline{P_\downarrow(\infty)} \simeq \frac{\sqrt{\pi}b}{4\sqrt{2}\sigma\delta h_z} e^{b^2/(8\sigma^2\delta h_z^2)} \text{erfc}\left(\frac{b}{2\sqrt{2}\sigma\delta h_z}\right), \quad (13)$$

which is similar to the ESR result, except that the nuclear fluctuations  $\sigma$  are replaced here by a reduced value  $\sigma\delta h_z$ . We have checked that Eq. (13) is in agreement with direct numerical evaluation. As seen in Fig. 1(d), deviations from the ESR result exist in general but in the current experimental regime can be safely neglected, because they only become important when  $\eta \sim 1$ .

By considering the dependence of  $\overline{P_\downarrow(\infty)}$  on detuning, we can reach a similar conclusions about the EDSR linewidth. Like in regular ESR ( $\eta \rightarrow 0$  limit), a larger drive leads to a general increase of  $\overline{P_\downarrow(\infty)}$ , as well as a broadening of the linewidth. In principle, the effect of

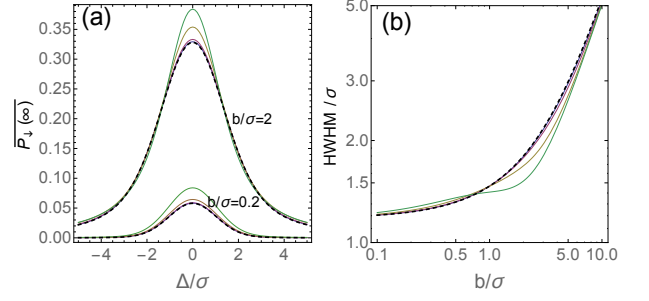


FIG. 2. Dependence of  $\overline{P_\downarrow(\infty)}$  on different system parameters, for several values of  $\eta = 0.05, 0.1, 0.2, 0.5, 1$ . For each family of curves, larger values of  $\eta$  correspond to larger deviations from the  $\eta = 0.05$  result (dashed curve), which is essentially indistinguishable from  $\eta = 0$ . In panel (a) we plot  $\overline{P_\downarrow(\infty)}$  as function of detuning, at two representative drive strengths  $b/\sigma = 0.2$  and 2. Panel (b) is a plot of the value of  $\Delta/\sigma$  which gives the half width at half-maximum, as a function of  $b/\sigma$ .

transverse fluctuations could modify the lineshape significantly. As shown in Fig. 2(a), at strong drive and  $\eta \sim 1$  the increase of  $\overline{P_\downarrow(\infty)}$  is mostly around  $\Delta = 0$ , which leads to a smaller value of the half width at half-maximum (HWHM). However, very small deviations from the Voigt profile occur for currently more typical values  $\eta \ll 1$ . The general features of the linewidth are summarized by Figs. 1(d) and 2(b), referring respectively to the height of the peak at  $\Delta = 0$  and the HWHM.

Our discussion of  $\overline{P_\downarrow(\infty)}$  thus indicates that common methods to estimate the value of  $\sigma$  are still valid for large-amplitude EDSR. Instead, the decay of Rabi oscillations is much more sensitive to the physical origin of the drive. One can see, contrasting panels (b) and (d) of Fig. 1, that significant deviations from the ESR decay appear at relatively small values of  $\delta R/\delta x$ , when  $\overline{P_\downarrow(\infty)}$  has not yet saturated to 1/2. Further insight on the role of longitudinal/transverse nuclear fluctuations can be gained by analyzing the time dependence at finite detuning, which we discuss next.

*Decay at finite detuning.* The Rabi oscillations as function of time and detuning are plotted in Fig. 3, where the significant effect of  $\Delta$  on the shape and timescale of the decay can be seen. In the strong drive regime, Eq. (9) provides an excellent approximation, as shown in Fig. 3(c). A first consequence is that the Rabi oscillations approach the “chevron” pattern of Fig. 3(a). Furthermore the decay time gets reduced at a finite  $\Delta$ , which is illustrated in Figs. 3(c) and (d).

The dependence of  $T_R$  on  $\Delta$  has a simple physical explanation, as it can be traced to the difference in strength between transverse and longitudinal nuclear fluctuations shown in Fig. 1(a). Since Eq. (4) implies that a finite detuning corresponds to a field along  $z$  in the rotating frame, the relevant component of the nuclear fluctuations

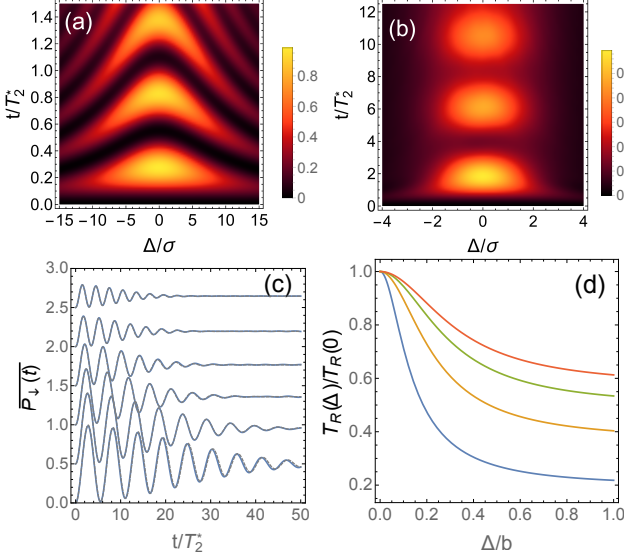


FIG. 3. Rabi oscillations at finite detuning. (a) and (b) are for  $\delta R/\delta x = 0.8$  and  $0.1$ , respectively. In both panels,  $\eta = 0.05$ . (c) shows the line cuts of (a) at  $\Delta/\sigma = 0, 2.5, 5, \dots, 12.5$  (bottom to top). For clarity, the curves are shifted vertically. The numerical results are virtually indistinguishable from Eq. (9), plotted as grey dashed curves. In panel (d) we plot Eq. (10) as function of detuning for several values of  $\delta R/\delta x = 0.4, 0.8, 1.2, 1.6$  (bottom to top).

(i.e., along the total driving field) becomes a weighted average of  $h_x$  and  $h_z$ . Since  $\delta h_z > \delta h_{xy}$ , the nuclear fluctuations gets enhanced by a finite detuning. As shown in Fig. 3(d), the dependence of  $T_R$  on  $\Delta$  is particularly pronounced at smaller values of  $\delta R/\delta x$ . This is natural, as the ratio  $\delta h_z/\delta h_{xy}$  is large in this regime, see Fig. 1(a), while the nuclear fluctuations become more isotropic at larger  $\delta R/\delta x$ . Thus, studying the dependence of  $T_R$  on  $\Delta$  allows one to explore how the relative strength of longitudinal/transverse nuclear fluctuations evolves with  $\delta R/\delta x$ .

*Comparison to experiments.* We now discuss the application of our theory to available experimental data. In Fig. 4 we show an analysis of the data shown in Fig. 2(c) of Ref. [9], obtained from InSb nanowire dots with strong spin-orbit interaction. As seen, our theory is able to reproduce well the Rabi oscillations and the fit yields values  $\delta R/\delta x$  and  $b$  consistent with  $b \propto \delta R/\delta x$ . For EDSR driven by the spin-orbit coupling we have:

$$\eta = \frac{l_{SO}}{2\delta x} \frac{\sigma}{\epsilon_z \sin \theta}, \quad (14)$$

where  $l_{SO}$  is the spin-orbit length and  $\theta$  the angle between the spin-orbit field and  $\vec{B}$ . Using  $l_{SO} = 200 - 300$  nm,  $\delta x \simeq 10 - 20$  nm [17],  $g = 41$ , and  $B = 31.4$  mT [9] gives  $\eta \simeq (0.015 - 0.04)/\sin \theta$ . Figure 4(b) implies  $\eta \sim 0.03$ , which is consistent with this estimate.

While Fig. 4(b) has  $\delta R/\delta x \lesssim 0.1$ , we estimate that larger values of  $\delta R/\delta x$  were achieved in a recent exper-

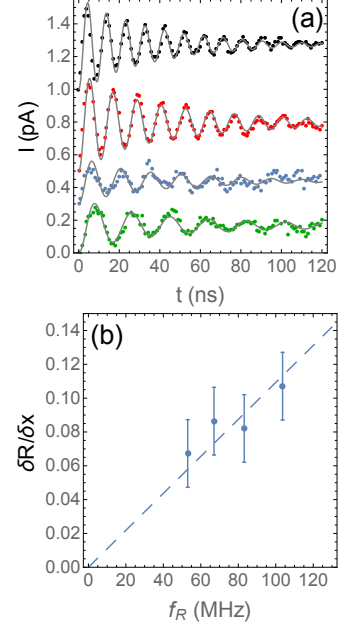


FIG. 4. (a): Fit of our theory to Rabi oscillations of Ref. [9]. For each curve, the fit parameters are  $\delta R/\delta x$ , a conversion factor to current, and  $b = 4\pi\hbar f_R$ , while  $\sigma = 0.22 \pm 0.03$   $\mu\text{eV}$  is from the experiment [9]. (b):  $\delta R/\delta x$  and  $f_R$  obtained from the fits in (a). The error bars are from the uncertainty on  $\sigma$ . The dashed line is a fit to  $\delta R/\delta x = C f_R$ .

iment on GaAs quantum dots [10]. There, the drive is based on a micromagnet for which numerical simulations give  $b/\delta R \sim |g|\mu_B \times (1 \text{ mT/nm})$  [10]. Using the largest achieved Rabi frequency  $f_{\text{max}} \sim 120$  MHz,  $|g| \simeq 0.4$ , and  $\delta x \sim 35 - 60$  nm (corresponding to orbital energies  $\sim 0.3 - 1$  meV), we obtain  $\delta R_{\text{max}}/\delta x \sim 0.7 - 1.2$  which is relatively close to the condition at which  $h_x$  fluctuations are most effective. On the other hand, the regime of motional narrowing  $\delta R/\delta x \gtrsim 1.8$  [18] does not appear to be within reach of current experiments. For GaAs quantum dots  $\sigma \sim |g|\mu_B \times (1 - 4 \text{ mT})$  [3, 11, 15, 19], which allows us to estimate a typical range  $\eta \sim 0.02 - 0.1$ .

Several findings of Ref. [10] are in good agreement with our discussion, including the transition to a “chevron” pattern in the strong drive regime [10]. As a result, our panels (a) and (b) of Fig. 3 are remarkably similar to the corresponding panels of Ref. [10]. Furthermore, a crossover from power-law decay (for  $b \lesssim |g|\mu_B \times 5$  mT) to gaussian decay (for  $b \gtrsim |g|\mu_B \times 15$  mT) was observed. The strength of the drive for such crossover is compatible with Eq. (12), which can be rewritten as  $b \gtrsim \sqrt{2\sigma\delta x}(b/\delta R) \sim |g|\mu_B \times (8 - 20 \text{ mT})$ , using the above estimates of  $\sigma, \delta x$ , and  $b/\delta R$ . We also show in Fig. 1(c) that Eq. (11) is able to reproduce the dependence of  $T_R$  on the drive strength, with reasonable fit parameters for GaAs quantum dots ( $T_2^* \simeq 9$  ns,  $\eta \simeq 0.09$ ). Our working assumption that nuclear fluctuations are the domi-

nant source of dephasing could be further tested through a detailed analysis of  $T_R$  as function of both drive and detuning, as it is unlikely that other dephasing mechanisms would have the same type of sensitive dependence discussed in relation to Fig. 3.

In conclusion, we have characterized the dephasing induced by the hyperfine interaction in large-amplitude EDSR, and showed that transverse fluctuations of the Overhauser field are likely to play an important role in recent experiments. From a general point of view, our study helps to assess fundamental limitations to spin manipulation due to the quantum-dot motion and the nuclear-spin bath. These two aspects are unavoidable for EDSR based on III-V semiconductors, in contrast to ESR or spin manipulation based on group-IV materials [20, 21].

We thank W. A. Coish, T. Otsuka, P. Stano, and J. Yoneda for discussions. D. L. acknowledges support from the Swiss NSF and NCCR QSIT.

---

\* stefano.chesi@csrc.ac.cn

- [1] R. Hanson, J. R. Petta, S. Tarucha, and L. M. K. Vandersypen, *Rev. Mod. Phys.* **79**, 1217 (2007).
- [2] D. D. Awschalom, L. C. Bassett, A. S. Dzurak, E. L. Hu, and J. R. Petta, *Science* **339**, 1174 (2013).
- [3] F. H. L. Koppens, C. Buizert, K. J. Tielrooij, I. T. Vink, K. C. Nowack, T. Meunier, L. P. Kouwenhoven, and L. M. Vandersypen, *Nature (London)* **442**, 766 (2006).
- [4] D. Loss and D. P. DiVincenzo, *Phys. Rev. A* **57**, 120 (1998).
- [5] V. N. Golovach, M. Borhani, and D. Loss, *Phys. Rev. B* **74**, 165319 (2006).
- [6] K. C. Nowack, F. H. L. Koppens, Y. V. Nazarov, and L. M. K. Vandersypen, *Science* **318**, 1430 (2007).
- [7] Y. Tokura, W. G. van der Wiel, T. Obata, and S. Tarucha, *Phys. Rev. Lett.* **96**, 047202 (2006).
- [8] M. Pioro-Ladrière, T. Obata, Y. Tokura, Y.-S. Shin, T. Kubo, K. Yoshida, T. Taniyama, and S. Tarucha, *Nature Phys.* **4**, 776 (2008).
- [9] J. W. G. van den Berg, S. Nadj-Perge, V. S. Pribiag, S. R. Plissard, E. P. A. M. Bakkers, S. M. Frolov, and L. P. Kouwenhoven, *Phys. Rev. Lett.* **110**, 066806 (2013).
- [10] J. Yoneda, T. Otsuka, T. Nakajima, T. Takakura, T. Obata, M. Pioro-Ladrière, H. Lu, C. J. Palmstrøm, A. C. Gossard, and S. Tarucha, *Phys. Rev. Lett.* **113**, 267601 (2014).
- [11] F. H. L. Koppens, D. Klauser, W. A. Coish, K. C. Nowack, L. P. Kouwenhoven, D. Loss, and L. M. K. Vandersypen, *Phys. Rev. Lett.* **99**, 106803 (2007).
- [12] S. Nadj-Perge, S. M. Frolov, E. P. A. M. Bakkers, and L. P. Kouwenhoven, *Nature* **468**, 1084 (2010).
- [13] E. I. Rashba, *Phys. Rev. B* **78**, 195302 (2008).
- [14] For an infinite temperature nuclear bath, we can always choose the drive along  $x$  in spin space due to the rotational invariance of the hyperfine coupling in the  $x - y$  plane, see Eq. (3). The strength of the drive is  $b_{\perp} = \sqrt{b_x^2 + b_y^2} = b$  if  $b_z = 0$ . If  $b_z \neq 0$ , one should substitute  $b \rightarrow b_{\perp}$  in Eq. (4) and in the rest of the paper.
- [15] E. A. Laird, C. Barthel, E. I. Rashba, C. M. Marcus, M. P. Hanson, and A. C. Gossard, *Phys. Rev. Lett.* **99**, 246601 (2007).
- [16] G. Széchenyi and A. Pályi, *Phys. Rev. B* **89**, 115409 (2014).
- [17] S. Nadj-Perge, V. S. Pribiag, J. W. G. van den Berg, K. Zuo, S. R. Plissard, E. P. A. M. Bakkers, S. M. Frolov, and L. P. Kouwenhoven, *Phys. Rev. Lett.* **108**, 166801 (2012).
- [18] For  $\delta R/\delta x \ll 1$ , the large-amplitude motion induces an averaging of several independent nuclear configurations, separated by a distance  $\sim \delta x$  [16]. This in turn leads to a decrease of  $\delta h_{xy}$ .
- [19] J. R. Petta, A. C. Johnson, J. M. Taylor, E. A. Laird, A. Yacoby, M. D. Lukin, C. M. Marcus, M. P. Hanson, and A. C. Gossard, *Science* **309**, 2180 (2005).
- [20] M. Veldhorst, J. C. C. Hwang, C. H. Yang, A. W. Leenstra, B. de Ronde, J. P. Dehollain, J. T. Muhonen, F. E. Hudson, K. M. Itoh, A. Morello, and A. S. Dzurak, *Nature Nanotechnology* **9**, 981 (2014).
- [21] E. Kawakami, P. Scarlino, D. R. Ward, F. R. Braakman, D. E. Savage, M. G. Lagally, M. Friesen, S. N. Coppersmith, M. A. Eriksson, and L. M. K. Vandersypen, arXiv:1404.5402 (2014).